Quantifying Earth's radiogenic heat budget

Laura Sammon[1,1] and William F McDonough[1,1]

[1]University of Maryland

November 30, 2022

Abstract

Earth's internal heat drives its dynamic engine, causing mantle convection, plate tectonics, and the geodynamo. These renewing and protective processes, which make Earth habitable, are fueled by a primordial (kinetic) and radiogenic heat. For the past two decades, particle physicists have measured the flux of geoneutrinos, electron antineutrinos emitted during β - decay. These ghost-like particles provide a direct measure of the amount of heat producing elements (HPE: Th & U) in the Earth and in turn define the planet's absolute concentration of the refractory elements. The geoneutrino flux has contributions from the lithosphere and mantle. Detector sensitivity follows a 1/r 2 (source detector separation distance) dependence. Accordingly, an accurate geologic model of the Near-Field Lithosphere (NFL, closest 500 km) surrounding each experiment is required to define the mantle's contribution. Because of its proximity to the detector and enrichment in HPEs, the local lithosphere contributes 50% of the signal and has the greatest effect on interpreting the mantle's signal. We re-analyzed the upper crustal compositional model used by Agostini et al. (2020) for the Borexino experiment. We documented the geology of the western Near-Field region as rich in potassic volcanism, including some centers within 50 km of the detector. In contrast, the Agostini study did not include these lithologies and used only a HPE-poor, carbonate-rich, model for upper crustal rocks in the surrounding 150 km of the Borexino experiment. Consequently, we report 3× higher U content for the local upper crust, which produces a 200% decrease in Earth's radiogenic heat budget, when compared to their study. Results from the KamLAND and Borexino geoneutrino experiments are at odds with one another and predict mantle compositional heterogeneity that is untenable. Combined analyses of the KamLAND and Borexino experiments using our revised local models strongly favor an Earth with 20 TW present-day total radiogenic power. The next generation of geoneutrino detectors (SNO+, counting; and JUNO, under construction) will better constrain the HPE budget of the Earth.

Quantifying Earth's radiogenic heat budget

Laura G. Sammon[a], William F. McDonough[a,b]

[a]Geology Department, 8000 Regents Drive, College Park, 20742, Maryland, USA
[b]Department of Earth Sciences and Research Center for Neutrino Science, Aoba-6-3 Aramaki, Aoba Ward, Sendai, 980-8577, Miyagi Prefecture, Japan

Abstract

Earth's internal heat drives its dynamic engine, causing mantle convection, plate tectonics, and the geodynamo. These renewing and protective processes, which make Earth habitable, are fueled by a primordial (kinetic) and radiogenic heat. For the past two decades, particle physicists have measured the flux of geoneutrinos, electron antineutrinos emitted during β^- decay. These ghost-like particles provide a direct measure of the amount of heat producing elements (HPE: Th & U) in the Earth and in turn define the planet's absolute concentration of the refractory elements. The geoneutrino flux has contributions from the lithosphere and mantle. Detector sensitivity follows a 1/r^2 (source detector separation distance) dependence. Accordingly, an accurate geologic model of the Near-Field Lithosphere (NFL, closest 500 km) surrounding each experiment is required to define the mantle's contribution. Because of its proximity to the detector and enrichment in HPEs, the local lithosphere contributes ~50% of the signal and has the greatest effect on interpreting the mantle's signal.

We re-analyzed the upper crustal compositional model used by Agostini et al. (2020) for the Borexino experiment. We documented the geology of the western Near-Field region as rich in potassic volcanism, including some centers within 50 km of the detector. In contrast, the Agostini study did not include these lithologies and used only a HPE-poor, carbonate-rich, model for upper crustal rocks in the surrounding ~150 km of the Borexino experiment. Consequently, we report 3× higher U content for the local upper crust, which produces a 200% decrease in Earth's radiogenic heat budget, when compared to their study. Results from the KamLAND and Borexino geoneutrino experiments are at odds with one another and predict mantle compositional heterogeneity that is untenable. Combined analyses of the KamLAND and Borexino experiments using our revised local models strongly favor an Earth with ~20 TW present-day total radiogenic power. The next generation of geoneutrino detectors (SNO+, counting; and JUNO, under construction) will better constrain the HPE budget of the Earth.

Keywords: Geoneutrino, crust, composition, modeling
PACS: 0000, 1111
2000 MSC: 0000, 1111

1. Introduction

A combination of primordial and radiogenic energy drives Earth's engine, with the former coming from planetary accretion and the latter from decay of K, Th, and U. Our planetary vehicle lacks a fuel gauge to define the amount of fuel left to power plate tectonics, mantle convection, and the geodynamo. Defining the thermal evolution of the planet gives insights into the cooling and crystallization history of the core, the temporal variation in mantle viscosity, and the nature of the cosmic building blocks of the Earth. With the dawn of geoneutrino detection [1], we now have the opportunity to define the Earth's radiogenic fuel budget, which in turn can specify the proportional contribution of these heat producing elements (K, Th, U) in the crust and mantle.

Twenty years have passed since particle physicists began detecting the Earth's emission of geoneutrinos (chargeless and near-massless particles emitted during β^- decay) [1]. The first generation of detectors (KamLAND in Japan and Borexino in Italy) have reported their flux measurements and interpreted their data in the context of an assumed geological model. The precision of the flux measurement (σ) continues to improve with exposure time, as it follow counting statistics ($\sigma \sim 1/\sqrt{N}$, N=number of observed events). The accuracy of the interpretation and its uncertainties depends on the assumed geological model. To interpret the geoneutrino flux measurement, one uses a detailed assessment of the Th and U abundances and distribution in the lithosphere surrounding the detector (closest ~500 km, which typically contributes 40 to 50% of the measured signal). A reference model is assumed for contributions from the remaining global lithosphere and mantle, with the Earth's core having negligible quantities of K, Th, and U, and no significant contribution to the signal. Combined analyses of the results from the KamLAND and Borexino experiments favor an Earth with ~20 TW present-day total radiogenic power (or a ~16 TW Earth for just Th and U power) [2, 3]. This finding indicates that ~40% of the Earth's estimated power of 46 ± 3 TW [4] comes from radiogenic sources.

Controversy remains, however, regarding the assumed geological model used to describe the local lithospheric contribution to the geoneutrino flux. For the lithosphere surrounding the KamLAND detector the various geological models predicting the local 3D distribution of Th and U differ by a factor of 1.4, based on their reported geoneutrino fluxes [5, 6, 7]. In contrast, for the Borexino detector the various predictions differ by a factor of 3 [8, 6, 9, 7]. The interpretation of the regional geology is important for geoneutrino studies as it fundamentally influences the final result, and the global abundances of Th and U.

The latest interpretation of geoneutrino data from the Borexino experiment [9] predicts a low contribution from their local crust to the overall geoneutrino signal. Consequently, their inferred mantle geoneutrino signal is high (~25 TW from Th+U), as well as their calculation for the bulk Earth's radiogenic power (~38 TW from K+Th+U), with model uncertainties at ~34% [9]. This prediction contrasts with other geoneutrino experiments [10, 11] and numerous geochemical [12, 13, 6, e.g.] and geophysical [14, 15, e.g.] models for Earth. Agostini et al. (2020)[9] places their upper limit of uncertainty at 51 TW of radiogenic heat production, which is outside of all geological observations.

Here we review the data for constructing a local geological model for the lithosphere immediately surrounding the Borexino detector. We evaluate the local geological model used in Agostini et al. (2020)[9] and compare it with competing models. We then test whether such models are consistent with the known regional geology and heat flux constraints. Using these findings, we identify the best local lithospheric models for the Borexnio experiment. Relying on the same principles, we discuss the competing local lithospheric models for the next generation of geoneutrino experiments.

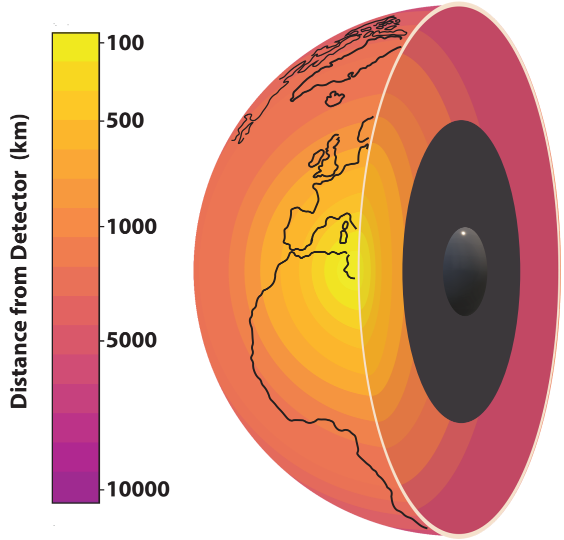

Figure 1: The strength of a geoneutrino signal depends on the abundance of the emitter (Th or U), and the 1/distance^2 from the emitted to the detector, regardless of direction. A detector in central Italy (Borexino) sees the strongest signal (yellow) from its immediate surrounding geology and the weakest signal from the opposite side of Earth (pink). The outer and inner core do not contribute to the geoneutrino signal and are grayed-out.

2. Background

Neutrinos are weakly-interacting fundamental particles that stream freely through matter, carrying information about their decay source. Detection of electron antineutrinos ($\bar{\nu}_e$) is accomplished via the Inverse Beta Decay (IBD) reaction with a free protons (p): $\bar{\nu}_e + p \rightarrow e^+ + n$ [n, neutron; e^+, positron] with an energy threshold of $E^{thr}_{\bar{\nu}_e} = 1.8$ MeV. This restriction allows detection of only the highest energy antineutrinos produced during some of the β^- decays in the ^{238}U and ^{232}Th decay chains [1].

Earth's total geoneutrino emission comes from the lithosphere and mantle, with the number of $\bar{\nu}_e$ observed (i.e., S, signal) by physicists is therefore:

$$S_{total} = S_{lithosphere} + S_{mantle} \tag{1}$$

S_{total} is reported in Terrestrial Neutrino Units (TNU) to normalize between detectors of different sizes; 1 TNU equals 1 antineutrino detection per 1 kiloton of scintillation fluid (10^{32} free protons) per year of exposure in a 100% efficient detector. S_{total} is proportional to the concentration of U and Th divided by the square of their distance (r) from the detector:

$$S_{total} \propto \frac{[U] + [Th]}{r^2} \tag{2}$$

Figure 1 shows the sensitivity of S_{total} relative to distance from the detector in central Italy. At a known decay rate, a relatively constant $(^{232}Th/^{238}U)_{molar}$ value [16], and an assumed K/U value, we calculate the abundance of the heat producing elements (K, Th, and U; HPEs). Please refer to Supplementary equation S1-Eq1 for the full calculation of the total $\bar{\nu}_e$ signal.

Compositional variations in the local lithosphere have the strongest effect on the geoneutrino signal because the lithosphere is closer to the detector (smaller r) and is 100-fold enriched in HPE relative to the mantle. Although the Earth's mantle is largest silicate reservoir, its low U concentration (≤10 ng/g) and distance (greater r) causes its signal to be muted.

To determine the contribution of geoneutrinos from the mantle, and therefore how much radioactive heat is left to power mantle convection, plate tectonics, or the geodynamo, we must first determine the U and Th concentrations in the lithosphere surrounding the detector. Subtracting the lithospheric signal from the total signal is done to establish the mantle value and its Th and U content. The $S_{lithosphere}$ has Near-Field Lithospheric (NFL) and Far-Field Lithospheric (FFL) contributions. Thus, the mantle geoneutrino signal is:

$$S_{mantle} = S_{total} - (S_{NFL} + S_{FFL}) \tag{3}$$

The relative contributions of these components are: Near-Field lithosphere (40 to 50%), Far-Field lithosphere (30 to 40%, i.e., global lithospheric signal), and mantle (≤25%) [7]. The lithosphere includes the mechanically coupled, underlying lithospheric mantle, which has limited compositional variation [17] and contributes little (order ~1 TNU, <10% of the signal) to the lithospheric signals [6]. Araki et al. [1] observed that the first 50 km and 500 km from KamLAND contributes ~25% and ~50%, respectively, of the total signal.

Modeling uncertainties: The relative uncertainties on the flux measurement at KamLAND and Borexino experiments improve over time; KamLAND went from ~54% to ~15% uncertainty for its measured flux, while Borexino went from ~42% to ~19%. The modern mantle with depleted and enrich domains is predicted to show only ~10% total variation in its geoneutrino signal [18]. Likewise, only ~10% relative variation is observed in estimates of the Far-Field lithospheric signal. Typically, the upper crust (i.e., the top 1/3 of the crust) contributes ~70% of the geoneutrino signal from the lithosphere. Hence, the greatest impact on interpreting the mantle signal comes from accurately predicting the upper crustal composition, that is, the S_{NFL}.

3. Lithospheric Modeling

Disentangling the mantle's contribution to S_{total} is a major goal of geoneutrino studies. Doing so requires accurate models for $S_{Lithosphere}$. Importantly, uncertainties (statistical and systematic) in the NFL model contribute most significantly to uncertainties in the modern mantle and global results.

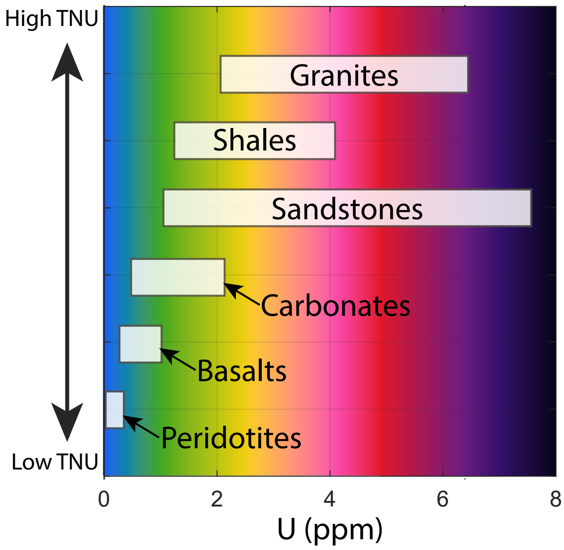

Figure 2: The average and range of U (and Th) depends on rock lithology. Granites tend to have higher average HPE content while carbonates and mafic rocks have lower averages. Sandstones, on the other hand, can have a wide range of U content depending on their formation and surrounding rocks. The white bar for each rock type shows the interquartile range of U concentrations from the Earthchem.org Database `https://www.earthchem.org`. See text for the definition of TNU.

Given the limited (±10%) variation in the mantle's signal, one expects its predicted values from different geoneutrino experiments to agree at this level. However, the local estimates of the modern mantle S_{mantle} range from ~30±13 TNU (power from K, Th, and U) by the Borexino team [9] to ~7±1.6 TNU by the KamLAND team [10]. Consequently, the disparate nature of these findings either means (1) the mantle is grossly heterogeneous (i.e., beyond scales envisaged by geology), or (2) there are substantial inaccuracies in lithospheric modeling.

The distribution, volume, composition (HPE content), and petrology of the formations surrounding a detector must be accurately determined for its contribution to S_{NFL}. Shales and granites are enriched in HPEs, whereas peridotites and carbonates normally are not. However, the degree of HPE enrichment is variable even within a given rock type. HPE concentrations differ among igneous, metamorphic, and sedimentary rocks, and between silicate and carbonate lithologies (Figure 2). It is therefore crucial to model accurately the proportional contribution of each geological formation and its HPE content near a detector.

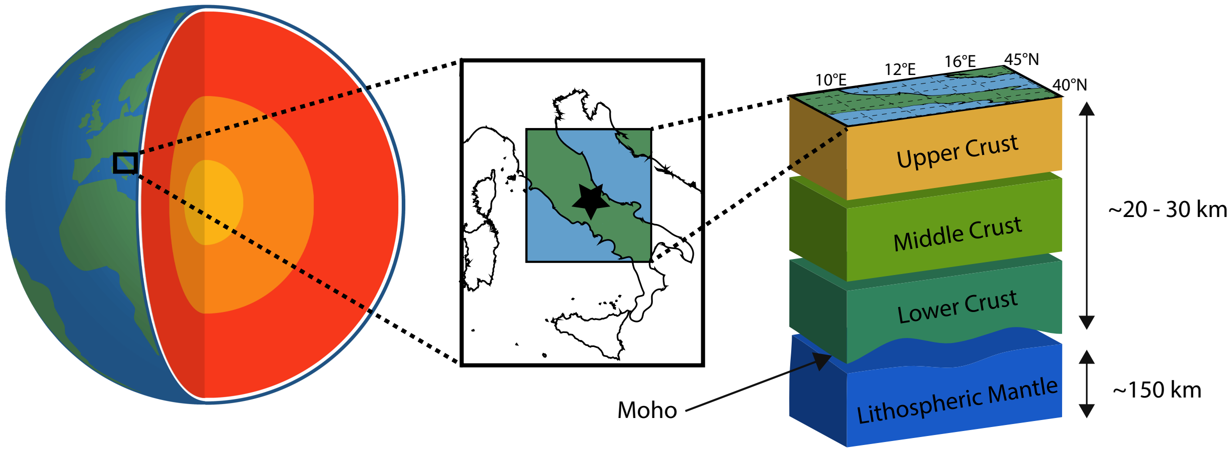

Figure 3: A schematic drawing of the location of the Borexino experiment and its Near-Field lithosphere (NFL; highlighted colored map in the center). Though the global abundance of U and Th contribute to the measured geoneutrino signal, the (continental) crust immediately surrounding the detector has the strongest effect on the signal.

The Borexino geoneutrino experiment at Gran Sasso National Laboratory was located outside of L'Aquila, Italy, in the central Italian peninsula (Figure 3, 13.57°E, 42.45°N, with 1.4 km of rock overburden). The Apennines consist primarily of foreland basin sediments and siliciclastic foredeep basin sediments, covered by Middle Pleistocene to Recent volcanics (on the western side) and continental shelf and marine deposits [19, 20]. The marine deposits are mainly dolomitic (marble, where metamorphosed). Extensional forces from mantle spreading to the west of the Apennines have led to a fault-block system of grabens filled with terreginous sediments in a region known as the Tyrrhenian Extensional Zone [19]. As a result, the uppermost crust near the detector could contain a mixture lithologies ranging from < 1 ppm to > 4 ppm U (Figure 2).

3.1. Near-Field and Far-Field Lithosphere

The Near-Field Lithosphere (NFL) is oftentimes, for the sake of computational ease, treated as the 4°latitude × 6°longitude area centered on the detector [6], rather than a circle with a 500 km diameter. The Far-Field Lithosphere (FFL) consists of the rest of the Earth's lithosphere (oceanic and continental). The crucial step, which requires geoscientific expertise, is determining the concentration and distribution of HPEs in the lithologies of the Near-Field Lithosphere.

S_{FFL} is a global average of the continental and oceanic lithospheric contribution to a detector's farfield geoneutrino flux. Model predictions for the S_{FFL} at existing and future planned detector sites are consistent, with estimates agreeing at better than the ±20% level. The competing predictions for ${}^{Borexino}S_{FFL}$ agree at 16±1 TNU [8, 6, 9, 7].

Whether a signal is from a moderate source of heat producing elements in the lithosphere near the detector or from a more concentrated mantle source is where discrepancies are introduced. To illustrate this point, and to highlight the need for accurate lithospheric models for the area surrounding geoneutrino detectors, we walk through the impacts of two different scenarios of upper crustal concentrations for Th and U near the Borexino geoneutrino detector.

Figure 4 illustrates the signal trade-off between HPE content of the Near-Field Lithosphere and mantle. S_{total} depends on the total mass of HPEs and their distance from the detector. The non-uniqueness of the modeling drives us to construct more accurate 3D descriptions of the HPE contents of the Near-Field Lithosphere, to evaluate better the mantle HPE concentrations.

3.2. Numerical Model

Figure 5 presents two NFL models used to analyze the effects of vastly different abundances of Th and U in the upper crust surrounding the Borexino detector: (1) a low Th+U content (e.g., dominantly carbonate) and (2) medium Th+U content (e.g.,shale-like, or averaged carbonate + siliciclastics + volcanic). These idealized models are comparable to those reported in (1) Agostini et al. [9] and Coltorti et al. [8], and (2) Huang et al. [6], Wipperfurth et al. [7], and McDonough et al. [2].

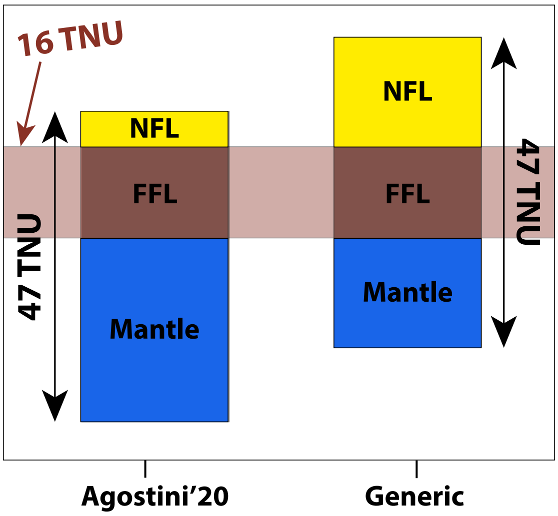

Figure 4: The total geoneutrino signal, S_{total} (length of the boxes in the figure) measured at a given detector remains relatively constant over time; the uncertainty decreases as the number of geoneutrino events detected increases. The amount of signal attributed to the Near-Field Lithosphere (NFL, yellow) determines how much signal must come from the mantle (blue). The average signal of the Far-Field Lithosphere (FFL, brown) generally stays the same (i.e., 16±1 TNU for Borexino).

Using Monte Carlo numerical modeling [7], we determined the expected ${}^{Borexino}S_{NFL}$ assuming two different scenarios: low and medium HPE contents for the upper crust. The HPE content of the middle, and lower crust and lithospheric mantle are taken from [21, 22]. For the physical description of the local lithosphere, we use the LITHO1.0 model [23] (i.e. density, distance from detector) with 1°latitude x 1°longitude horizontal resolution for the upper, middle, and lower crust and lithospheric mantle. Table 1 lists the compositional model parameters for the NFL, its signal, and that for the total lithosphere and mantle. This table also reveals the predicted power of the mantle and bulk Earth for these two different upper crustal models and thus NFL models.

A factor of three difference in the HPE budget of the upper crust for these two NFL models produces a factor of ~2 difference in both the estimated mantle and bulk Earth radiogenic power (Figure 6). These gross differences in the predicted radiogenic power demonstrate the significance of producing an accurate NFL model.

4. Importance of the Near-Field Lithosphere Model

The Apennines of the central Italian peninsula exposes a geological paradox across its eastern and western divide. Its Adriatic eastern side is composed of a compressional fold and thrust belt, whereas its Tyrrhenian western side is composed of extensional fault-block mountains. The paradox of this mountain belt is the juxtaposition of both compressional and extensional tectonic forces over a relatively narrowed (~150 km) east-west traverse.

Figure 7 shows that carbonate sediments surround the Borexino detector, whereas the western half of the Near-Field region exposes extensive deposits of Neogene to Quaternary igneous rocks [24, 25]. The Tuscan and Roman magmatic provinces are exposed all throughout the Tyrrhenian side of the Apennines and coastal plains. This western portion of the Italian peninsula is enriched in K, Th, and U, with some rocks containing as much as 25 μg/g U [26], which is slightly less than 10 times enriched over average upper crustal rocks [27].

These western Tuscan and Roman magmatic rocks are HPE-enriched and make up a significant portion of the upper crust of the NFL. Some of these rocks are within 50 km of the Borexino detector and need to be incorporated into any NFL model, but unfortunately these lithologies were not discussed by [8, 9]. Agostini et al. [9] highlighted the central tile, which includes the area within ~100 km of the Borexino detector and noted "Up to a distance of ~150 km from Borexino, 100% of the geoneutrino signal is generated from the LOC [local lithosphere]." Nearly all of the volcanoes identified in Figure 7, some of which are enormous volcanic centers, are within 150 km of the Borexino detector. In addition, the CROP 11 seismic refraction line that the Agostini et al. model cites as evidence for 13 km of carbonate sediments shows thick layers of siliciclastic sediments as well (e.g., [29, 30]).

To develop our alternative model of the ^{Borexino}NFL, we followed the practices of Huang et al. [6] and McDonough et al. [2] and used a generic, average upper crust composition [27]. Using such a generic model for the upper crust of the NFL results in a mantle and bulk Earth model that is consistent with studies that favor a 20 TW radiogenic Earth [2, 3].

Disparities between the predicted HPE concentrations in the upper crust for the NFL cause the greatest systematic uncertainties in calculated radiogenic heat production. Constructing a purely carbonate versus a generic upper crust around the detector changes the expected mantle radiogenic heat budget from 30 TW to 13 TW, respectively. These contrasting models illustrate the consequences of modeling different proportions of HPE lithologies for the NFL. Consequently, inaccurate estimates of the subsurface composition near a detector vastly change the implications of the observed geoneu-

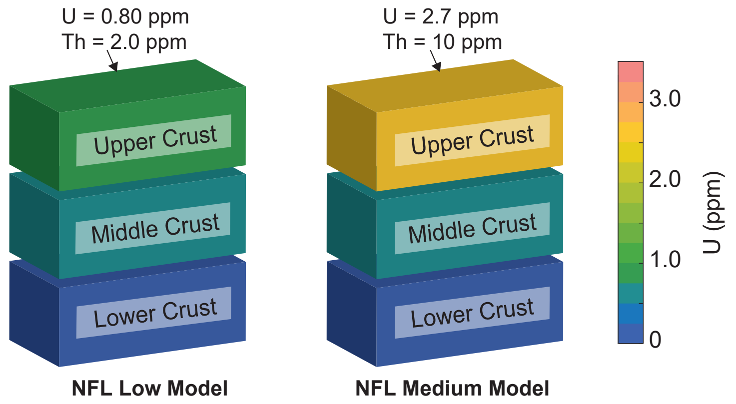

Figure 5: Two different Near-Field Lithosphere models illustrate low (Agostini'20) and medium (Generic) U and Th scenarios in the uppermost crust near our geoneutrino detector. The middle and lower crust are kept the same among the three models since we are primarily interested in the effects of upper crustal compositional changes. See [6] for discussions on middle/lower/deep crustal geoneutrino contributions.

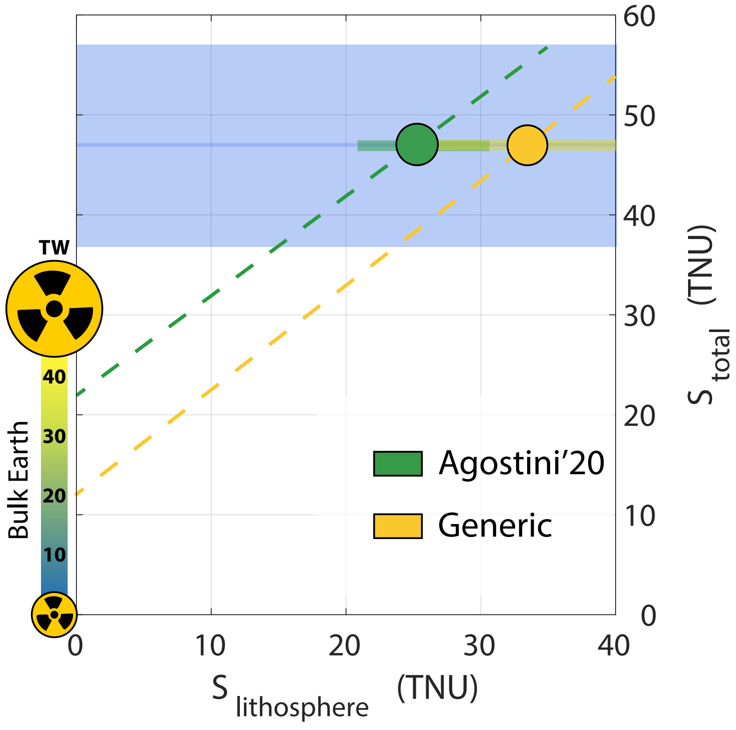

Figure 6: The lithospheric geoneutrino signal (predicted, $S_{lithosphere}$) vs. the measured geoneutrino signal (S_{total}) for the Agostini et al. model and Generic Model introduced in Table 1. The Agostini et al. Model has a smaller predicted bulk lithospheric signal, attributing $25.9^{+4..9}_{-4.1}$ TNU for U and Th. The Generic model has a higher concentration of U and Th in the upper crust of the NFL, and therefore a greater bulk lithospheric flux, $32.3^{+7.9}_{-6.4}$ TNU. The dashed lines with slopes = 1 show the y-intercept for each model. The y-intercept is the S_{mantle}. The blue-shaded area shows the Borexino measured S_{total} of $47^{+10.8}_{-9.6}$ TNU (with the signal errors including the sum of statistical and systematic uncertainties).

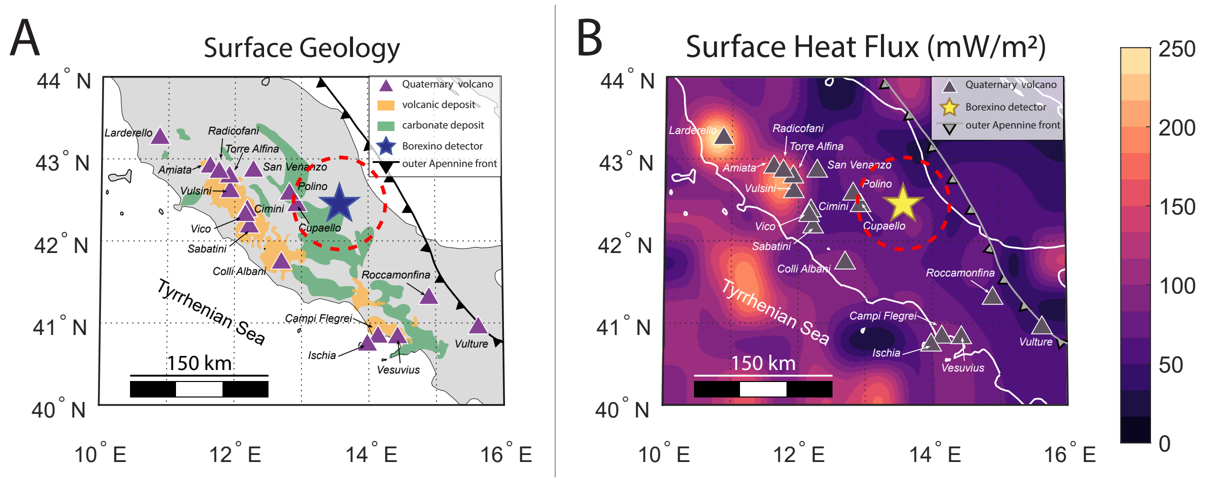

Figure 7: A simplified geological map (A) of the central Italian peninsula showing extensive volcanism on the western portion and carbonate platforms to the east (modified after [19, 26]). The red dashed line circles the Borexino detector (blue star) at a radius of 50 km. Quaternary volcanic deposits in the west coincide with high surface heat flux (B). Heat flux data from [28]

trino signal S_{total}.

5. Heat Flux Constraints on Lithospheric Models

To further assess the upper crustal model of the ^{Borexino}NFL we turned to the available heat flux data for the central Apennines [31, 32]. Given the regional tectonic setting discussed above, it is not surprising to observe a clear distinction between the western, high heat flux (>150 mW/m^2) and the eastern low heat flux (<70 mW/m^2) provinces [31] (Figure 7). Moreover, using observable crustal radiogenic heat production data, Verdoya et al. (2001)[32] concluded that low surface heat flux estimates (e.g., values <45 mW/m^2) are unreliable in the Apennines. This study also concluded that the central Apennines region has an average heat flux of ~70 mW/m^2 (with eastern and western limbs being approximately 55 and 150 mW/m^2, respectively). On average, the ^{Borexino}NFL has a relatively normal continental surface heat flux value (e.g., ~63 mW/m^2, [28]).

Surface heat flux is the sum of contributions from heat production in the crust and the heat flux across the Moho. The total surface heat flux (Total$_{HF}$) can be expressed as the sum of crustal and Moho heat fluxes:

$$Total_{HF} \equiv Crust_{HF} + Moho_{HF} \tag{4}$$

Normally, a regionally averaged surface heat flux (e.g., ~63 mW/m^2) is dominated by an upper crustal fraction (i.e., 50 to 60%) and, less so, by a ~1/3 contribution from the Moho heat flux (i.e, 21 ± 10 mW/m^2) [22]. If we assume a generic crustal compositional model (Table 1), the regional Total$_{HF}$ for the Italian peninsula appears normal in terms of its heat production and surface heat flux (i.e., ~70 mW/m^2). In contrast, assuming the compositional model for the NFL adopted by Agostini'20 [8] puts the Crust$_{HF}$ contribution at 24 mW/m^2 and a Moho$_{HF}$ of 46 mW/m^2 – more than double the global average. While this level of Moho heat flux is possible, it is only observed in areas of recent volcanism, which contradicts the low HPE carbonate shelf model.

The Agostini et al. (2020) model for the mantle's radiogenic heat (30 TW) is also inconsistent with their choice of a 8.1 TW global lithosphere model. The Earth has 46 ± 3 TW of heat [15], which is both radiogenic and primordial in origin, with other contributions including 3 TW from oceanic hot spots [33, 34], 0.4 TW from tidal heating, crust-mantle differentiation, and thermal contraction [34], and a minimum of 6 TW to 12 TW from secular cooling of the mantle [35]. Consequently, for Agostini et al.'s (2020) accounting to be correct, it leaves anywhere from -2 to -8 TW for the core-mantle boundary (CMB) heat flux, meaning that the mantle is radiating 2 to 8 TW of heat into Earth's core as it heats up over time. Our alternative model has $7.6^{+2.1}_{-1.6}$ TW for the global lithosphere [7] and 12.9 TW in the mantle. This model yields a CMB heat flux of 10 to 16 TW, in agreement with estimates from previous studies [33, 36, 37, 38, 39].

The first experiment to detect geoneutrinos, KamLAND, in Kamioka, Japan, predicts a low radiogenic power Earth, $11.2^{+7.9}_{-5.1}$ TW for Th and U only, or 14 TW when including the decay of other isotopes [10]. This result is intermediate between the low H (H = heat production) estimates for the Earth [13] and middle H estimates [12, 40]. The NFL model used by the KamLAND team [41] predicts an Earth with a low radiogenic power, whereas that proposed by Wipperfurth et al. [7] predicts an Earth with 20 TW of total radiogenic power.

These KamLAND results challenge the Earth model of Agostini et al. (2020) that predicts 38 TW of radiogenic power. Either (1) the geological compositions of the KamLAND and/or the Borexino models need to be thoroughly re-investigated, or (2) one would have to predict a hemispherical dichotomy in the mantle's composition. The latter hypothesis is, of course, unsupported by empirical data on the composition of mid-ocean ridge basalts and ocean island basalts. The second hypothesis seems completely untenable.

In summary, we document the significance of geology's input into interpreting the particle physics flux data. The combined results for KamLAND and Borexino experiments strongly favor a 20 TW radiogenic Earth model. Moreover, these results confirm that the bulk Earth has a 1.9× enrichment in refractory elements over a CI chondritic composition [42].

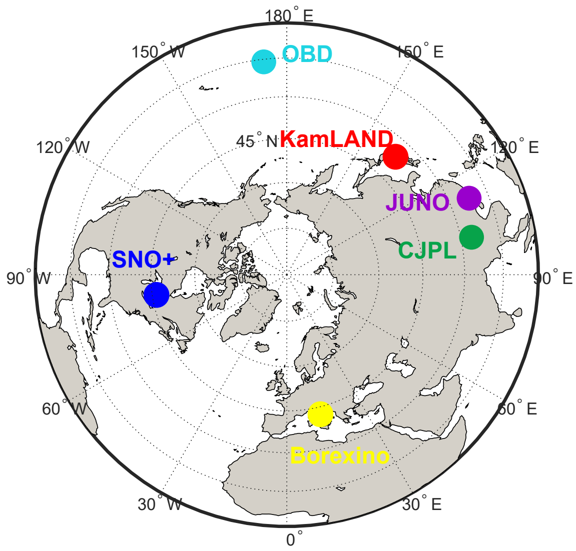

Figure 8: Borexino and KamLAND will be joined by the next generation of geoneutrino detectors, including SNO+, which is already counting, and JUNO, which is under construction. The under-development CJPL detector next to the Himalayas marks the fifth detector in the northern hemisphere, allowing for unprecedented mantle resolution. The OBD (ocean bottom detector) experiment is a mobile device and its position can be optimized as being 3000 km away from South America, Australia, and the core mantle boundary.

6. The Future of Neutrino Geoscience

High resolution crustal models accounting for the specific types and proportions of lithologies surrounding each geoneutrino detector must be constructed to interpret geoneutrino flux measurement. The geology underlying active geoneutrino detectors (Figure 8) in Gran Sasso, Italy, Kamioka, Japan, and Sudbury, Canada, reveal complicated tectonic features (e.g., (paleo-)subduction and synorogenic extension, ocean-continent subduction zone, large impact structure). Geoneutrino data already exists from two of these locations, but these crustal models are either low resolution or in conflict with one another. We must reconcile the geoneutrino signal at each location with improved local and regional geology. We must use a wide range of independent geoscientific data to constrain the composition of the NFL. Moreover, our compositional models needs to be internally consistent with available heat flow, geochemistry/petrology, structural geology, and seismology data to reduce the systematic uncertainties on Earth's HPE content and thermal budget.

There three more geoneutrino projects under construction or development: Jiangmen Underground Neutrino Observatory (JUNO, Figure 8 purple dot) in south-eastern China, which will be 20x larger than any existing detector [43]; China Jinping Underground Laboratory (CJPL, Figure 8 green dot) sited on the eastern slope of the Tibetan plateau and Himalayan ramp and at 2.4 km depth [44]; and OBD, a movable, Ocean Bottom Detector (Figure 8 teal dot) proposed by a team of scientists and engineers working with JAMSTEC [45]. These projects each represent massive feats of engineering and decades-long data collection experiments and require substantial geoscientific input.

The decay of HPEs contribute substantially to Earth's internal heat. By quantifying Earth's geoneutrino flux, we can precisely establish how much fuel from HPEs is left to power mantle convection and the recycling processes of plate tectonics. Geoneutrinos studies use modern physics technology to measure directly and instantaneously the current compositional properties of the inaccessible mantle. Th and U exist in Earth in constant, chondritic ratios to 26 other elements [12]; if we constrain the abundance of HPEs, we can establish Earth's concentrations of Ca, Al, Nb, and the economically valuable rare earth elements. With the second generation of geoneutrino detectors on the horizon, geoscientists and physicists are poised to unravel Earth's heat budget from the tallest mountains to the bottom of the oceans.

Table 1: Borexino Models for the upper crust in the NFL, bulk calculated Signal, and Radiogenic Power

		Agostini'20	Generic	Units
UC†	K	9,600	23,200	μg/g
	Th	2.0	10.5	μg/g
	U	0.8	2.7	μg/g
	HP‡	0.16	0.62	nanoW/kg
Signal	S_{NFL}	9.7	16.6	TNU
	S_{FFL}	16.3	15.7	TNU
	S_{Mantle}	21.2	14.7	TNU
R* Heat	Mantle	30	13	TW
	Total	38	20	TW

UC† local model for the Upper Continental Crust. NFL = Near-Field Lithosphere (i.e., closest ~500 km to a detector). Units: μg/g (10^{-6} kg/kg); TNU (Terrestrial Neutrino Unit, see text for details); TW (Terra Watts, 10^{12} watts). R* radiogenic power. HP‡ Heat Production.

7. Conclusion

The power of geoneutrino studies lies in directly quantifying the amount of heat producing elements in the bulk Earth. Deep reservoirs in Earth that before were unreachable are being sampled by particle physicists, but these studies have not reached a consensus on what their results mean for mantle heat production. The geoneutrino signal at a given detector is a combination of crust-sourced and mantle-sourced Th and U decays. Since geoneutrinos do not carry directional information, the lithospheric signal must be constrained to quantify the mantle's abundances of Th and U.

Approximately 50% of the geoneutrino signal is produced from the Near-Field Lithosphere (NFL), with 25% of the signal coming from the HPEs within 50 km of the detector. Conflicting Near-Field Lithospheric compositional models lead to profoundly different consequences for the predicted HPE content in the mantle and Earth's thermal evolution.

The Borexino particle physics team [9] modeled the NFL surrounding their detector as predominantly carbonate, with low concentrations of Th and U. Their model therefore requires most of the geoneutrino signal to come from the distant mantle, implying a 30 TW of mantle radiogenic heat production. Consequently, >80% of all of the Earth's internal heat is radiogenic. This high heat production mantle is inconsistent with measurements from the detector at KamLAND and with heat flux observations.

Alternatively, the inclusion of Neogene to Recent, HPE-rich volcanic deposits in the Borexino NFL region results in a more normal average upper crustal composition for Th and U. Using this upper crustal model (versus a low HPE model) can explain the Borexino signal, resulting in 13 TW of radiogenic power in the mantle or a 20 TW radiogenic Earth. It is therefore imperative to produce high-resolution NFL maps with accurate proportions of each HPE lithology.

The direct measurement of geoneutrinos can provide crucial insights into the sources and distribution of heat producing elements in the Earth. When paired with accurate geological knowledge, these high-energy antineutrinos emitted from HPE decays within Earth helps establish the composition of the planet's building blocks as well as the fuel left to power Earth's dynamic interior.

8. Author Contributions

LGS and WFM contributed to the conceptualization of this project. LGS constructed the synthetic models. LGS and WFM wrote and edited this manuscript together. All authors have read and approved this manuscript

9. Acknowledgments

LGS and WFM gratefully acknowledge the NSF for support (grants EAR1650365 and EAR2050374) and University of Maryland for a Wiley fellowship. Both authors would also like to acknowledge Jordan Goldstein, who worked with them to create the figures and schematics in this paper. The authors also thank Fabio Mantovani for his edits and suggestions.

References

[1] T. Araki, S. Enomoto, K. Furuno, Y. Gando, K. Ichimura, H. Ikeda, K. Inoue, Y. Kishimoto, M. Koga, Y. Koseki, et al., Experimental investigation of geologically produced antineutrinos with KamLAND, Nature 436 (7050) (2005) 499–503. doi:https://doi.org/10.1038/nature03980.

[2] W. F. McDonough, O. Šrámek, S. A. Wipperfurth, Radiogenic power and geoneutrino luminosity of the earth and other terrestrial bodies through time, Geochemistry, Geophysics, Geosystems 21 (7) (2020) e2019GC008865. doi:https://doi.org/10.1029/2019GC008865.

[3] G. Bellini, K. Inoue, F. Mantovani, A. Serafini, V. Strati, H. Watanabe, Geoneutrinos and geoscience: an intriguing joint-venture, La Rivista del Nuovo Cimento (2021) 1–105doi:https://doi.org/10.1007/s40766-021-00026-7.

[4] C. Jaupart, S. Labrosse, F. Lucazeau, J.-C. Mareschal, Temperatures, heat, and energy in the mantle of the earth, in: G. Schubert (Ed.), Treatise on Geophysics (Second Edition), Vol. 7, Elsevier, Oxford, 2015, pp. 223–270. doi:10.1016/B978-0-444-53802-4.00126-3.

[5] S. Enomoto, Experimental study of geoneutrinos with KamLAND, in: Neutrino Geophysics: Proceedings of Neutrino Sciences 2005, Springer, 2006, pp. 131–146. doi:https://doi-org.proxy-um.researchport.umd.edu/10.1007/978-0-387-70771-6_9.

[6] Y. Huang, V. Chubakov, F. Mantovani, R. L. Rudnick, W. F. McDonough, A reference Earth model for the heat-producing elements and associated geoneutrino flux, Geochemistry, Geophysics, Geosystems 14 (6) (2013) 2003–2029. doi:10.1002/ggge.20129.

[7] S. A. Wipperfurth, O. Šrámek, W. F. McDonough, Reference models for lithospheric geoneutrino signal, Journal of Geophysical Research: Solid Earth 125 (2) (2020) e2019JB018433. doi:https://doi.org/10.1029/2019JB018433.

[8] M. Coltorti, R. Boraso, F. Mantovani, M. Morsilli, G. Fiorentini, A. Riva, G. Rusciadelli, R. Tassinari, C. Tomei, G. Di Carlo, et al., U and Th content in the central Apennines continental crust: A contribution to the determination of the geo-neutrinos flux at LNGS, Geochimica et Cosmochimica Acta 75 (9) (2011) 2271–2294. doi:10.1016/j.gca.2011.01.024.

[9] M. Agostini, K. Altenmüller, S. Appel, V. Atroshchenko, Z. Bagdasarian, D. Basilico, G. Bellini, J. Benziger, D. Bick, G. Bonfini, D. Bravo, B. Caccianiga, F. Calaprice, A. Caminata, L. Cappelli, P. Cavalcante, F. Cavanna, A. Chepurnov, K. Choi, D. D'Angelo, S. Davini, A. Derbin, A. Di Giacinto, V. Di Marcello, X. F. Ding, A. Di Ludovico, L. Di Noto, I. Drachnev, G. Fiorentini, A. Formozov, D. Franco, F. Gabriele, C. Galbiati, M. Gschwender, C. Ghiano, M. Giammarchi, A. Goretti, M. Gromov, D. Guffanti, C. Hagner, E. Hungerford, A. Ianni, A. Ianni, A. Jany, D. Jeschke, S. Kumaran, V. Kobychev, G. Korga, T. Lachenmaier, T. Lasserre, M. Laubenstein, E. Litvinovich, P. Lombardi, I. Lomskaya, L. Ludhova, G. Lukyanchenko, L. Lukyanchenko, I. Machulin, F. Mantovani, G. Manuzio, S. Marcocci, J. Maricic, J. Martyn, E. Meroni, M. Meyer, L. Miramonti, M. Misiaszek, M. Montuschi, V. Muratova, B. Neumair, M. Nieslony, L. Oberauer, A. Onillon, V. Orekhov, F. Ortica, M. Pallavicini, L. Papp, O. Penek, L. Pietrofaccia, N. Pilipenko, A. Pocar, G. Raikov, M. T. Ranalli, G. Ranucci, A. Razeto, A. Re, M. Redchuk, B. Ricci, A. Romani, N. Rossi, S. Rottenanger, S. Schönert, D. Semenov, M. Skorokhvatov, O. Smirnov, A. Sotnikov, V. Strati, Y. Suvorov, R. Tartaglia, G. Testera, J. Thurn, E. Unzhakov, A. Vishneva, M. Vivier, R. B. Vogelaar, F. von Feilitzsch, M. Wojcik, M. Wurm, O. Zaimidoroga, S. Zavatarelli, K. Zuber, G. Zuzel, Comprehensive geoneutrino analysis with Borexino, Phys. Rev. D 101 (1) (2020) 012009. doi:10.1103/PhysRevD.101.012009.

[10] A. Gando, Y. Gando, H. Hanakago, H. Ikeda, K. Inoue, K. Ishidoshiro, H. Ishikawa, M. Koga, R. Matsuda, S. Matsuda, et al., Reactor on-off antineutrino measurement with KamLAND, Physical Review D 88 (3) (2013) 033001. doi:https://doi.org/10.1103/PhysRevD.88.033001.

[11] M. Agostini, S. Appel, G. Bellini, J. Benziger, D. Bick, G. Bonfini, D. Bravo, B. Caccianiga, F. Calaprice, A. Caminata, P. Cavalcante, A. Chepurnov, K. Choi, D. D'Angelo, S. Davini, A. Derbin, L. Di Noto, I. Drachnev, A. Empl, A. Etenko, G. Fiorentini, K. Fomenko, D. Franco, F. Gabriele, C. Galbiati, C. Ghiano, M. Giammarchi, M. Goeger-Neff, A. Goretti, M. Gromov, C. Hagner, T. Houdy, E. Hungerford, A. Ianni, A. Ianni, K. Jedrzejczak, M. Kaiser, V. Kobychev, D. Korablev, G. Korga, D. Kryn, M. Laubenstein, B. Lehnert, E. Litvinovich, F. Lombardi, P. Lombardi, L. Ludhova, G. Lukyanchenko, I. Machulin, S. Manecki, W. Maneschg, F. Mantovani, S. Marcocci, E. Meroni, M. Meyer, L. Miramonti, M. Misiaszek, M. Montuschi, P. Mosteiro, V. Muratova, B. Neumair, L. Oberauer, M. Obolensky, F. Ortica, K. Otis, L. Pagani, M. Pallavicini, L. Papp, L. Perasso, A. Pocar, G. Ranucci, A. Razeto, A. Re, B. Ricci, A. Romani, R. Roncin, N. Rossi, S. Schönert, D. Semenov, H. Simgen, M. Skorokhvatov, O. Smirnov, A. Sotnikov, S. Sukhotin, Y. Suvorov, R. Tartaglia, G. Testera, J. Thurn, M. Toropova, E. Unzhakov, R. B. Vogelaar, F. von Feilitzsch, H. Wang, S. Weinz, J. Winter, M. Wojcik, M. Wurm, Z. Yokley, O. Zaimidoroga, S. Zavatarelli, K. Zuber, G. Zuzel, Spectroscopy of geoneutrinos from 2056 days of Borexino data, Phys. Rev. D 92 (2015) 031101. doi:10.1103/PhysRevD.92.031101.

[12] W. F. McDonough, S.-S. Sun, The composition of the Earth, Chemical geology 120 (3-4) (1995) 223–253. doi:https://doi.org/10.1016/0009-2541(94)00140-4.

[13] M. Javoy, E. Kaminski, F. Guyot, D. Andrault, C. Sanloup, M. Moreira, S. Labrosse, A. Jambon, P. Agrinier, A. Davaille, C. Jaupart, The chemical composition of the Earth: Enstatite chondrite models, Earth and Planetary Science Letters 293 (3) (2010) 259–268. doi:10.1016/j.epsl.2010.02.033.

[14] D. Turcotte, G. Schubert, Geodynamics (3rd Edition), Cambridge University Press, 2014.

[15] C. Jaupart, J.-C. Mareschal, L. Iarotsky, Radiogenic heat production in the continental crust, Lithos 262 (2016) 398–427. doi:https://doi.org/10.1016/j.tecto.2012.12.001.

[16] S. A. Wipperfurth, M. Guo, O. Šrámek, W. F. McDonough, Earth's chondritic Th/U: Negligible fractionation during accretion, core formation, and crust–mantle differentiation, Earth and Planetary Science Letters 498 (2018) 196–202. doi:10.1016/j.epsl.2018.06.029.

[17] W. F. McDonough, Constraints on the composition of the continental lithospheric mantle, Earth and Planetary Science Letters 101 (1) (1990) 1–18. doi:https://doi.org/10.1016/0012-821X(90)90119-I.

[18] O. Šrámek, W. F. McDonough, E. S. Kite, V. Lekić, S. T. Dye, S. Zhong, Geophysical and geochemical constraints on geoneutrino fluxes from Earth's mantle, Earth and Planetary Science Letters 361 (2013) 356–366. doi:10.1016/j.epsl.2012.11.001.

[19] D. Cosentino, P. Cipollari, P. Marsili, D. Scrocca, Geology of the central Apennines: a regional review, Journal of the virtual explorer 36 (11) (2010) 1–37. doi:10.3809/jvirtex.2010.00223.

[20] G. Vignaroli, M. Mancini, F. Bucci, M. Cardinali, G. P. Cavinato, M. Moscatelli, M. Putignano, P. Sirianni, M. Santan-

gelo, F. Ardizzone, et al., Geology of the central part of the Amatrice Basin (Central Apennines, Italy), Journal of Maps 15 (2) (2019) 193–202. doi:https://doi.org/10.1080/17445647.2019.1570877.

[21] L. G. Sammon, W. F. McDonough, A geochemical review of amphibolite, granulite, and eclogite facies lithologies: Perspectives on the deep continental crust, Journal of Geophysical Research: Solid Earth (2021) e2021JB022791.

[22] L. G. Sammon, W. F. McDonough, W. D. Mooney, The composition of the deep continental crust inferred from geochemical and geophysical data, Journal of Geophysical Research: Solid Earth (2022) *in review*doi:https://doi.org/10.1002/essoar.10507582.1.

[23] M. E. Pasyanos, T. G. Masters, G. Laske, Z. Ma, LITHO1.0: An updated crust and lithospheric model of the Earth, Journal of Geophysical Research: Solid Earth 119 (3) (2014) 2153–2173. doi:10.1002/2013JB010626.

[24] A. Lima, S. Albanese, D. Cicchella, Geochemical baselines for the radioelements K, U, and Th in the Campania region, Italy: a comparison of stream-sediment geochemistry and gamma-ray surveys, Applied Geochemistry 20 (3) (2005) 611–625. doi:https://doi.org/10.1016/j.apgeochem.2004.09.017.

[25] M. Xhixha, M. Baldoncini, G. Bezzon, G. Buso, L. Carmignani, L. Casini, I. Callegari, T. Colonna, S. Cuccuru, E. Guastaldi, et al., A detailed gamma-ray survey for estimating the radiogenic power of Sardinian Variscan crust, NORM & Environmental Radioactivity 45 (2014) 70–74.

[26] S. Conticelli, R. W. Carlson, E. Widom, G. Serri, Chemical and isotopic composition (Os, Pb, Nd, and Sr) of Neogene to Quaternary calc-alkalic, shoshonitic, and ultrapotassic mafic rocks from the Italian peninsula: Inferences on the nature of their mantle sources, Cenozoic volcanism in the Mediterranean area 418 (2007) 171.

[27] R. L. Rudnick, S. Gao, Composition of the Continental Crust, in: Treatise on Geochemistry, Elsevier, 2014, pp. 1–51. doi:10.1016/B978-0-08-095975-7.00301-6.

[28] F. Lucazeau, Analysis and mapping of an updated terrestrial heat flow data set, Geochemistry, Geophysics, Geosystems 20 (8) (2019) 4001–4024. doi:https://doi.org/10.1029/2021JB022791.

[29] E. Patacca, P. Scandone, E. Di Luzio, G. P. Cavinato, M. Parotto, Structural architecture of the central Apennines: Interpretation of the CROP 11 seismic profile from the Adriatic coast to the orographic divide, Tectonics 27 (3) (2008). doi:https://doi.org/10.1029/2005TC001917.

[30] E. Di Luzio, G. Mele, M. Tiberti, G. Cavinato, M. Parotto, Moho deepening and shallow upper crustal delamination beneath the central Apennines, Earth and Planetary Science Letters 280 (1-4) (2009) 1–12. doi:https://doi.org/10.1016/j.epsl.2008.09.018.

[31] C. Pauselli, G. Gola, P. Mancinelli, E. Trumpy, M. Saccone, A. Manzella, G. Ranalli, A new surface heat flow map of the Northern Apennines between latitudes 42.5 and 44.5°N, Geothermics 81 (2019) 39–52. doi:https://doi.org/10.1016/j.geothermics.2019.04.002.

[32] M. Verdoya, P. Chiozzi, G. Gola, Unravelling the terrestrial heat flow of a young orogen: The example of the northern Apennines, Geothermics 90 (2021) 101993. doi:https://doi.org/10.1016/j.geothermics.2020.101993.

[33] S. Labrosse, J.-P. Poirier, J.-L. Le Mouël, The age of the inner core, Earth and Planetary Science Letters 190 (3-4) (2001) 111–123. doi:https://doi.org/10.1016/S0012-821X(01)00387-9.

[34] C. Jaupart, S. Labrosse, F. Lucazeau, J. Mareschal, 7.06-Temperatures, heat and energy in the mantle of the Earth, Treatise on geophysics 7 (2007) 223–270.

[35] S. Labrosse, Core-mantle boundary, heat flow across, in: D. Gubbins, E. Herrero-Bervera (Eds.), Encyclopedia of Geomagnetism and Paleomagnetism, Springer, Dordrecht, 2007, pp. 127–130. doi:https://doi.org/10.1007/978-1-4020-4423-6_51.

[36] S. Labrosse, Hotspots, mantle plumes and core heat loss, Earth and Planetary Science Letters 199 (1-2) (2002) 147–156. doi:https://doi.org/10.1016/S0012-821X(02)00537-X.

[37] P. H. Roberts, C. A. Jones, A. R. Calderwood, Energy fluxes and ohmic dissipation in the Earth's core, Earth's core and lower mantle (2003) 100–129.

[38] J. Korenaga, Plate tectonics, flood basalts and the evolution of earth's oceans, Terra Nova 20 (6) (2008) 419–439. doi:https://doi.org/10.1111/j.1365-3121.2008.00843.x.

[39] T. Nakagawa, P. J. Tackley, Influence of initial cmb temperature and other parameters on the thermal evolution of earth's core resulting from thermochemical spherical mantle convection, Geochemistry, Geophysics, Geosystems 11 (6) (2010). doi:https://doi.org/10.1029/2010GC003031.

[40] H. Palme, H. S. C. O'Neill, Cosmochemical estimates of mantle composition, in: R. W. Carlson (Ed.), The Mantle and Core, Vol. 3 of *Treatise on Geochemistry (Second Edition)* of Treatise on Geochemistry (Second Edition), Elsevier, Oxford, 2014, Ch. 1, pp. 1–39, editors-in-chief H. D. Holland and K. K. Turekian. doi:10.1016/B978-0-08-095975-7.00201-1.

[41] S. Enomoto, E. Ohtani, K. Inoue, A. Suzuki, Neutrino geophysics with KamLAND and future prospects, Earth and Planetary Science Letters 258 (1-2) (2007) 147–159. doi:10.1016/j.epsl.2007.03.038.

[42] T. Yoshizaki, W. F. McDonough, Earth and Mars–distinct inner solar system products, Geochemistry 81 (2) (2021) 125746.

[43] F. An, G. An, Q. An, V. Antonelli, E. Baussan, J. Beacom, L. Bezrukov, S. Blyth, R. Brugnera, M. B. Avanzini, et al., Neutrino physics with JUNO, Journal of Physics G: Nuclear and Particle Physics 43 (3) (2016) 030401.

[44] J. F. Beacom, S. Chen, J. Cheng, S. N. Doustimotlagh, Y. Gao, G. Gong, H. Gong, L. Guo, R. Han, H.-J. He, X. Huang, J. Li, J. Li, M. Li, X. Li, W. Liao, G.-L. Lin, Z. Liu, W. McDonough, O. Šrámek, J. Tang, L. Wan, Y. Wang, Z. Wang, Z. Wang, H. Wei, Y. Xi, Y. Xu, X.-J. Xu, Z. Yang, C. Yao, M. Yeh, Q. Yue, L. Zhang, Y. Zhang, Z. Zhao, Y. Zheng, X. Zhou, X. Zhu, K. Zuber, Physics prospects of the Jinping neutrino experiment, Chinese Physics C 41 (2) (2017) 023002. doi:10.1088/1674-1137/41/2/023002.

[45] T. Sakai, K. Inoue, H. Watanabe, W. F. McDonough, N. Abe, E. Araki, T. Kasaya, M. Kyo, N. Sakurai, K. Ueki, H. Yoshida, Study of Ocean Bottom Detector for observation of geo-neutrino from the mantle, Proceedings for TAUP (2022).

Supporting Information for " Quantifying Earth's radiogenic heat budget"

1. Full electron antineutrino flux equation

Table S1 explains the meaning of each symbol and its units.

$$\frac{dN(E_{\bar{\upsilon}_e}, \vec{r})}{d(E_{\bar{\upsilon}_e})} = \epsilon \, \frac{N_A \lambda}{\mu} \, \sigma_P \, (E_{\upsilon_e}) \, \frac{dn(E_{\bar{\upsilon}_e})}{d(E_{\bar{\upsilon}_e})} \int_{\oplus} P_{ee} \, (E_{\bar{\upsilon}_e}, |\vec{r} - \vec{r}\prime|) d\vec{r}\prime \, \frac{a(\vec{r})\rho(\vec{r}\prime)}{4\pi|\vec{r} \; - \; \vec{r}\prime|^2} \tag{1}$$

Table 1: Heat production and geoneutrino flux results

Symbol	Description	Units
$\frac{dN(E_{\bar{\upsilon}_e}, \vec{r})}{d(E_{\bar{\upsilon}_e})}$	$\bar{\nu}_e$ detection spectrum	$\bar{\nu}_e$
ϵ	10^{32} protons x 3.154 x 10^7s x 100%*	$proton \times s$
N_A	Avogadro's number	$\frac{atom}{mol}$
λ	Decay constant	$\frac{decay}{s \times atom}$
μ	Atomic mass	$\frac{kg}{mol}$
$\sigma_P \; (E_{\upsilon_e})$	$\bar{\nu}_e$ cross-section (function of $E_{\bar{\upsilon}_e}$)	$\frac{m^2}{proton}$
$\frac{dn(E_{\bar{\upsilon}_e})}{d(E_{\bar{\upsilon}_e})}$	$\bar{\nu}_e$ emission spectrum	$\frac{\bar{\nu}_e}{decay}$
$P_{ee} \; (E_{\bar{\upsilon}_e}, \vert\vec{r} \; - \; \vec{r}\prime\vert)$	Oscillation probability (function of $E_{\bar{\upsilon}_e}$)	unitless
$a(\vec{r})$	Concentration of radionuclide in cell	$\frac{kg}{kg}$
$\rho(\vec{r}\prime)$	Density of rock in cell	$\frac{kg}{m^3}$
$\vert\vec{r} \; - \; \vec{r}\prime\vert^2$	Distance from cell to detector	m

*detector size and efficiency normalization factor

2. Heat production from K, Th, and U decay

Table 2: Radionuclide heat production

Radionuclide	Mole Fraction (%)	λ (a^{-1})	Q(MeV)	Q(pJ)
^{232}Th	100	4.916 x 10^{-11}	42.646	6.8326
^{235}U	0.72049	9.8531 x 10^{-10}	46.397	7.4336
^{238}U	99.2740	1.5513 x 10^{-10}	51.694	8.2823
^{40}K	0.01167	5.491 x 10^{-10}*	1.331*	2.132*

*Total from all ^{40}K decay modes